

13,01

## Effect of High Temperature Annealing on the Physicochemical Properties of systems based on $\text{FeSi}_x$

© D.E. Nikolichev, R.N. Kriukov, A.V. Zdoroveyshchev, Yu.M. Kuznetsov, D.A. Zdoroveyshchev, Yu.A. Dudin, M.V. Dorokhin, A.A. Skrylev

Lobachevsky State University,  
Nizhny Novgorod, Russia

E-mail: nikolitchev@phys.unn.ru

Received December 6, 2022

Revised December 28, 2022

Accepted December 28, 2022

It has been established that the physicochemical properties of structures based on iron silicides formed by ion implantation of iron ions into silicon depend significantly on the time of subsequent high-temperature annealing. Objects with different geometric parameters are formed on the surface and the roughness increases. Annealing at  $1000^\circ\text{C}$  in an Ar atmosphere is accompanied by a decrease in the content of the Fe–Si chemical bonds during the first 60 seconds. The reason for the drop in thermal conductivity with increasing annealing temperature is the formation of silicide complexes.

**Keywords:** iron silicide, thermoelectric, ion implantation, chemical composition, X-ray photoelectron spectroscopy.

DOI: 10.21883/PSS.2023.03.55594.547

### 1. Introduction

The development of thermoelectric power converters is promising from the point of view of their potential application in various fields [1]. The use of thermoelectrics as power sources is hindered by the low efficiency factor. The efficiency of thermoelectric conversion of a material with electrical conductivity  $\sigma$  and thermal conductivity  $\chi$  at absolute temperature  $T$  and thermoelectric power factor  $\alpha$  is determined by the dimensionless thermoelectric  $QZT = (\alpha^2\sigma T)/\chi$ . Bismuth telluride with  $ZT \approx 1.0$  [1] currently has the best performance among industrial materials at room temperature. The main problem of raising  $ZT$  is to increase the efficiency of thermoelectric conversion when using materials with high electrical conductivity and low thermal conductivity, but their independent variation within the same material is almost impossible [2].

Interest in silicon compounds lies in its prevalence and ease of embedding such systems into existing circuits. Si compounds have a wide range of electrical properties. Therefore, the opportunity of creating thermoelectric converters based on it looks like an extremely urgent task.

The work considers  $\text{FeSi}_x$  compounds obtained by implantation of Fe ions into a silicon substrate followed by high-temperature annealing. Iron silicides are widely used in semiconductor electronics as optical, photonic devices, integrated electronic and spintronic systems [3–5]. These options are complemented by the opportunity of creating thermoelectric converters based on them. At the moment, for such materials, the value of  $ZT$  has been reached, equal to 0.4 and 0.2 for the electron and hole semiconductors, respectively [6]. The prospect of increasing  $ZT$  is seen in

the creation of a multiphase system based on heavily doped silicon with nano-inclusions of iron silicides [7], and the study of the chemical composition and physical properties is an urgent task.

### 2. Experimental part

This work has studied silicon structures with iron silicide inclusions formed by ion implantation and thermal annealing. The chemical composition of the structures was studied by X-ray photoelectron spectroscopy (XPS), supplemented by layer-by-layer ion etching. The work was carried out on an ultra-high vacuum complex Omicron Multiprobe RM. The emission of photoelectrons occurred under the influence of  $\text{MgK}\alpha$  radiation, and the PC lines of Fe  $2p$ , Si  $2s$ , Si  $2p$ , O  $1s$ , C  $1s$  were recorded. The diameter of the analyzed region was 3 mm. The layer-by-layer analysis of the structures was carried out by sputtering the layers with  $\text{Ar}^+$  ions with an energy of 1 keV. The angle between the ion beam and the sample surface was  $45^\circ$ . A protocol for chemical bond identification and quantification is provided in [8,9]. When analyzing the profile of the Fe  $2p$  PV line, it was found that in the  $\text{FeSi}_x$  compounds there are peaks of energy loss on plasmon oscillations with energy  $\sim 730$  eV [10], and the ratio of the intensities of the plasmon lines losses and the main doublet Fe  $2p$  is  $\sim 1 : 2$ . This feature allowed to estimate the concentration of chemical bonds Fe–Si.

At Si ion implantation, a KEF-5000 substrate with a thickness of  $500\ \mu\text{m}$  was irradiated with Fe ions with charges +1, +2 and +3 at an accelerating voltage of 80 kV at the

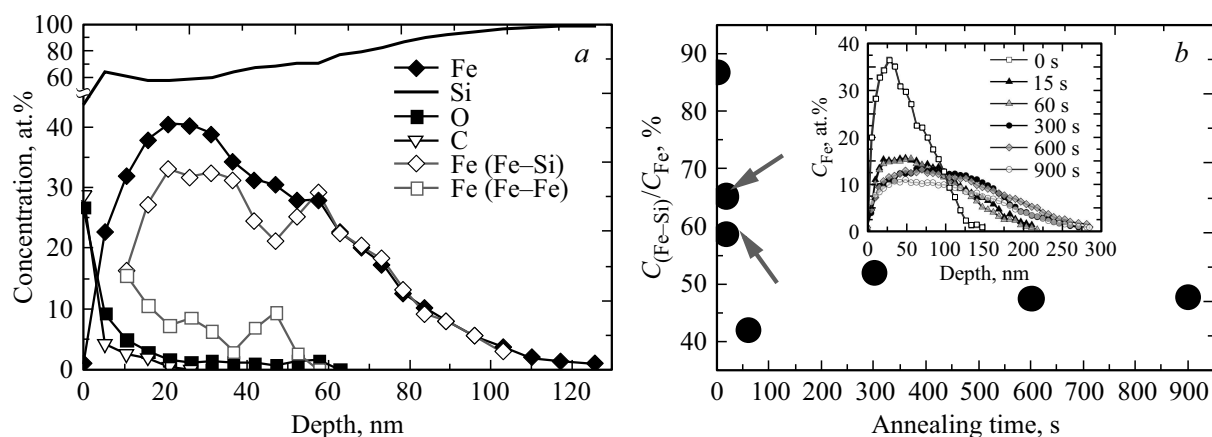


**Figure 1.** *a)* Deep distribution profile of the concentration of chemical elements and chemical bonds in iron-implanted silicon prior to annealing. *b)* Dependence of the ratio of the concentration of Fe in the chemical bond Fe–Si to the total Fe content in the system (arrows indicate Si:Fe samples annealed under the same conditions; percentage the ratio of areas under the distribution curves Fe–Si and Fe). Inset: distribution profiles of the relative concentration of iron obtained at different annealing times.

„Raduga 3“. The accumulated dose was  $5 \cdot 10^{16} \text{ cm}^{-2}$ . After ion implantation, the samples were annealed at  $1000^\circ\text{C}$  for 0, 15, 60, 300, 600, and 900 s in an Ar atmosphere in a Jipelec JetFirst200C fast thermal annealing unit.

The surface morphology of the samples was studied using a Solver Pro atomic-force microscope (AFM) in the semi-contact mode using HA NC (NT–MDT) probes. Scans  $50 \times 50 \mu\text{m}^2$  and  $7 \times 7 \mu\text{m}^2$  were registered.

The modified method  $3\omega$  [11] was used to measure the thermal conductivity. An  $\text{Al}_2\text{O}_3$  layer with a thickness of  $\sim 7 \text{ nm}$  was deposited on the surface of the samples, followed by a 3-nm Pd–Au layer. After that, a contact was formed in the form of a strip 3 mm long and  $20 \mu\text{m}$  wide using photolithography and etching the metal layer down to the dielectric. The dielectric thickness was chosen in such a way that, on the one hand, it provides good electrical insulation, and on the other — hand, it does not introduce a significant error into the measurement of the thermal conductivity coefficient. When an alternating electric current was passed through the contact using a Keithley 6221 programmable alternator, the frequency response of the voltage at a triple frequency was recorded using a Stanford SR810 Lock-In programmable selective voltmeter-amplifier. During the measurement, the sample was placed on a graphite furnace placed in a vacuum chamber with a pressure of  $10^{-3} \text{ Torr}$ , and the furnace was heated by a halogen lamp.

Since the working area for the thermoelectric power converter is the implanted layer, in order to eliminate the influence of the main silicon part of the sample, the frequency characteristics of two samples were sequentially recorded in the adapted technique: the sample with implanted iron and the initial substrate with the deposited  $\text{Al}_2\text{O}_3$  layer. The deposition of a dielectric on a high-resistance silicon substrate is due to the need to take into account its contribution to the thermal conductivity coefficient during measurements, and not to isolate the

contact from the substrate. To eliminate the systematic error, the  $\text{Al}_2\text{O}_3$  layer was deposited in a single technological cycle both on the substrate and on the sample with implanted iron.

### 3. Results and discussion

The iron implanted in silicon has an asymmetric distribution (Fig. 1, *a*) with a Fe content maximum at a 20 nm depth, which corresponds to the depth obtained in the calculation in the SRIM [p]rogram 12. Oxygen and carbon were detected only on the surface of the sample, which indicates the absence of pollutants in the ion source. In systems annealed for longer than 15 s, oxygen is drawn in to large depths, reaching 60–80 nm. Two samples annealed for 15 s reflect the reproducibility of the results (Fig. 1 *b*). Differences in the content are caused by the error of the XPS method and the possible heterogeneity of the current density of Fe ions in the beam. It is also worth pointing out the practically identical distribution profiles of the content of elements in structures annealed for 300 seconds or more, which indicates the depletion of thermally stimulated processes in the system already at 300 s (Fig. 1, *b*, inset). A significant increase in the width of the Fe profile is observed already at an annealing time of 60 s. Probably, annealing with a minimum duration is sufficient both for reduction of the crystal structure of the material after implantation and for the formation of  $\text{FeSi}_x$  nanocrystals. This is also seen in the distribution profiles of chemical bonds at depths of 15–40 nm (Fig. 1, *a*).

The distribution profiles of the chemical bond content of Fe, presented in Fig. 1, *a*, show that the near-surface region is enriched with iron in the elemental state. This can be explained by the displacement to the surface of metal atoms that are not embedded in the Si lattice. It can also be assumed that when a significant dose is reached, Fe atoms accumulate as clusters, the formation of which is confirmed

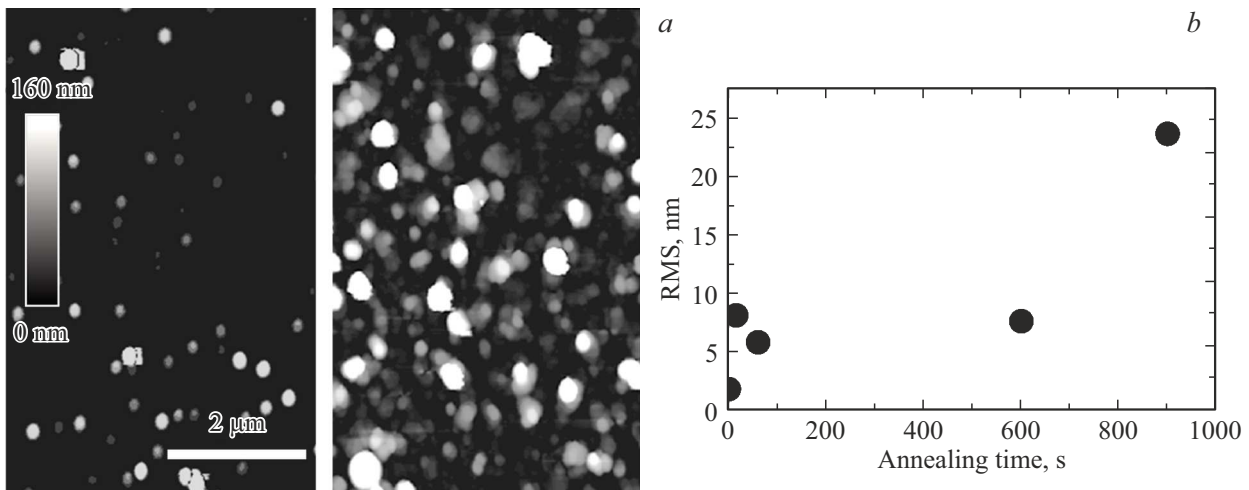


**Figure 2.** *a*) AFM images of the surface of the original sample (left) and the sample annealed for 900 s (right); *b*) dependence of roughness on annealing time.

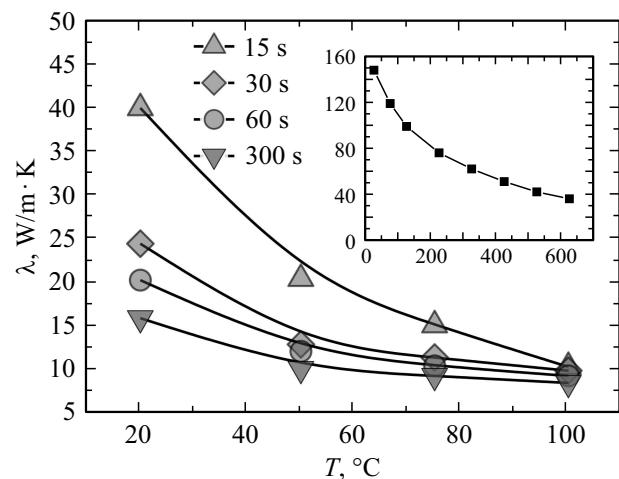
by the data of transmission electron microscopy [13]. This is probably due to the fast loss of energy by iron ions during a large number of their collisions with atoms of the radiation-damaged matrix.

Figure 1, *b* shows the dependence of the chemical bond fraction Fe–Si in the total iron content on the time of fast thermal annealing. It can be seen from the data that the maximum fraction of Fe, which is in combination with Si, is determined in the initial sample as 88%. Carrying out annealing with a duration of only 15 s leads to a sharp decrease in the concentration of Fe–Si. An increase in duration over 60 s does not lead to reliably determined changes in quantitative characteristics.

Changes in the properties of the Si:Fe system are accompanied by modification of the surface of the samples (Fig. 2, *a*). On the AFM images of the samples surface not subjected to annealing, micron-scale objects are recorded. With an increase in the annealing time, their number increases. The initial sample has a minimum roughness (Fig. 2, *b*), and the roughness reaches its maximum value at an annealing time of 900 s. The trend suggests a further increase in roughness with increasing annealing duration, and this indicates the absence of a relationship between surface processes and thermally stimulated diffusion of Fe in depth. As a result of the studies, the instability of the  $\text{FeSi}_x$  system obtained by implantation of Fe ions was revealed. This manifests itself in a reduction in the concentration of Fe atoms associated with Si during annealing at 1000°C.

The temperature dependences of the thermal conductivity (Fig. 3) show that as the annealing temperature increases, the value of the thermal conductivity of the structure decreases.

The inset in Fig. 3 shows the thermal conductivity of the initial silicon substrate with the  $\text{Al}_2\text{O}_3$  dielectric layer deposited on it, and it can be seen from a comparison of the values that the introduction of iron into silicon leads to a



**Figure 3.** Temperature dependence of the thermal conductivity of ion-synthesized  $\text{FeSi}_x$  structures annealed at a temperature of 1000°C for 15, 30, 60 and 300 s. Inset: dependence of the thermal conductivity of the initial Si substrate KEF-5000.

strong decrease in the thermal conductivity. This is probably due to the coalescence of iron silicide complexes near the surface, causing the effect of phonon mode blocking [1].

#### 4. Conclusion

An increase in the duration of annealing brings the system into equilibrium, and the ratio of the number of chemical bonds Fe–Si/Fe reaches a value of 1:1. Annealing stimulates the diffusion of Fe atoms deep into the Si substrate, and processes occur in the near-surface layers that lead to formations of micron and submicron sizes. During annealing in an argon atmosphere, despite the reduction of the crystal structure, the determining factor for the drop in

thermal conductivity is the formation of complexes of iron silicides and metal inclusions.

### Funding

The work was carried out as part of the implementation of the N-487-99 project under the program of strategic academic leadership „Priority-2030“.

### Conflict of interest

The authors declare that they have no conflict of interest.

### References

- [1] D.M. Rowe. Thermoelectrics Handbook. Macro to Nano. Boca Raton: CRC/Taylor & Francis, N.W. (2006). P. 28–91. <https://doi.org/10.1201/9781420038903>
- [2] Y.C. Dou, X.Y. Qin, D. Li, L.L. Li, T.H. Zou, Q.Q. Wang. J. Appl. Phys. **114**, 4, 044906 (2013). <https://doi.org/10.1063/1.4817074>
- [3] Q. Wan, T.H. Wang, C.L. Lin. Appl. Phys. Lett. **82**, 19, 3224 (2003). <https://doi.org/10.1063/1.1574845>
- [4] K. Yamaguchi, K. Shimura, H. Udono, M. Sasase, H. Yamamoto, S. Shamoto, K. Hojou. Thin Solid Films **508**, 1–2, 367 (2006). <https://doi.org/10.1016/j.tsf.2005.07.354>
- [5] I.A. Tarasov, M.A. Visotin, A.S. Aleksandrovsky, N.N. Kosyrev, I.A. Yakovlev, M.S. Molokeevev, A.V. Lukyanenko, A.S. Krylov, A.S. Fedorov, S.N. Varnakov, S.G. Ovchinnikov. J. Magn. Magn. Mater. **440**, 15, 144 (2017). <https://doi.org/10.1016/j.jmmm.2016.12.084>
- [6] H. Lange. Physica Status Solidi B **201**, 1, 3 (1997). DOI: 10.1002/1521-3951(199705)201:1;3::AID-PSSB3;3.0.CO;2-W
- [7] R. Fortulan, S.A. Yamini. Mater. **14**, 20, 6059 (2021). DOI: 10.3390/ma14206059
- [8] A.V. Boryakov, S.I. Surodin, R.N. Kryukov, D.E. Nikolichev, S.Yu. Zubkov. J. Electron Spectroscopy. Rel. Phenomena **229**, 132 (2018). <https://doi.org/10.1016/j.elspec.2017.11.004>
- [9] N. Ohtsu, M. Oku, A. Nomura, T. Sugawara, T. Shishido, K. Wagatsuma. Appl. Surf. Sci. **254**, 11, 3288 (2008). <https://doi.org/10.1016/j.apsusc.2007.11.005>
- [10] A.V. Sidashov, A.T. Kozakov, V.I. Kolesnikov, D.S. Manturov, S.I. Yaresko. J. Friction. Wear **41**, 6, 549 (2020). DOI: 10.3103/S1068366620060185
- [11] K. Maize, Y. Ezzahri, X. Wang, S. Singer, A. Majumdar, A. Shakouri. In: Twenty-fourth Annual IEEE Semiconductor Thermal Measurement and Management Symposium / Eds R. Wilcoxon, R. Collins. IEEE Service Center, Piscataway (2008). P. 185. DOI: 10.1109/STHERM.2008.4509388
- [12] <http://www.srim.org>
- [13] E.A. Chusovitin, S.V. Vavanova, I.A. Petrushkin, N.G. Galkin, R.M. Bayazitov, R.I. Batalov, G.D. Ivlev, T.S. Shamirzaev. Khim. fizika i mezoskopiya. (in Russian). **11**, 3, 374 (2009).

*Translated by E.Potapova*